https://doi.org/10.5194/wes-2026-108
Preprint. Discussion started: 6 July 2026
© Author(s) 2026. CC BY 4.0 License.

eawe european academy of wind energy
Open Access WIND ENERGY SCIENCE DISCUSSIONS

Sub-minute Fatigue Monitoring for Enhanced Lifetime Assessment of Wind Turbines

Catarina Oliveira[1,2], André Biscaya[3], João Santos[3], Elsa Caetano[1], Min Xu[2]

[1]CONSTRUCT, Faculty of Engineering, University of Porto, Rua Dr. Roberto Frias s/n, 4200-465 Porto, Portugal
[2]Structural Monitoring Unit, National Laboratory for Civil Engineering, Av. do Brasil 101, 1700-066 Lisbon, Portugal
[3]Innovation, AI, Data, and Analytics Department, Nadara, Rua João Chagas 53, Piso 5, 1495-072 Algés, Portugal

Correspondence to: Catarina Oliveira (up202111325@up.pt)

Abstract. Accurate fatigue damage estimation is a critical step for managing and extending the life of wind turbine fleets, and the basis on which operators decide whether an ageing asset can be kept in service beyond the end of design life. The most accurate estimation relies on continuous high-frequency strain measurements processed with rainflow cycle counting. However, the data volumes, computational complexity, and associated costs of doing this over long-term periods and across large fleets make it impractical at fleet scale. For this reason, industry practice has long relied on stress data aggregated over 10-minute windows already used by Supervisory Control and Data Acquisition (SCADA) systems. This choice is convenient but tends to underestimate fatigue damage generated by cycles whose period exceeds the windows, driven by slow variations in wind speed, operational transitions and control actions.

Technology has recently enabled operators to deploy second-resolution SCADA metrics at scale and at reasonable cost. This is an opportunity to revisit fatigue monitoring at a SCADA-aligned timescale that is short enough to retain the cycles a 10-minute window discards, yet aggregated enough to remain deployable across large fleets. This paper benchmarks the families of methods that make this opportunity actionable against continuous rainflow as a baseline: conventional window-based counting, a modified Low-Frequency Fatigue Dynamics (LFFD) formulation that explicitly resolves intra-window and inter-window damage contributions, and two reduced-information extrema-sequence representations — Start-Peaks-Valleys-End (SPVE) and Maximum and Minimum (Max–Min). The evaluation uses six months of 15-second windows of SCADA and strain measurements acquired at 50 Hz from two instrumented tower sections of an onshore wind turbine and examines the influence of window length, sampling rate, and fatigue-curve formulation on damage computation (Eurocode 3 *vs* DNV).

Reducing the aggregation window from 10-minute to 15-second alone does not improve fatigue estimation, as shorter windows increasingly truncate the low-frequency cycles that dominate accumulated damage. The proposed modified LFFD framework overcomes this limitation by preserving cycle continuity across window boundaries, recovering 99.5% of the baseline damage while requiring only a fraction of the original data volume. Reduced-information representations further demonstrate that fatigue can be estimated with high accuracy using strongly compressed stress sequences, with Start-Peaks-Valleys-End (SPVE) and Maximum and Minimum (Max–Min) retaining 98.8% and 96.2% of the baseline damage,

https://doi.org/10.5194/wes-2026-108
Preprint. Discussion started: 6 July 2026
© Author(s) 2026. CC BY 4.0 License.

eawe european academy of wind energy
Open Access WIND ENERGY SCIENCE DISCUSSIONS

respectively. These findings establish a practical pathway towards SCADA-aligned, data-efficient fatigue monitoring, enabling scalable lifetime assessment across large wind turbine fleets while preserving the fidelity of high-resolution structural measurements.

1 Introduction

Wind turbine structures are subjected to highly variable loading arising from stochastic aerodynamic forcing, control actions, grid interactions, and frequent transitions between operational states (IEC 61400-13, 2015; Pacheco et al., 2022; Pacheco, 2022). These excitations generate cyclic stresses in structural components, leading to progressive fatigue damage, one of the governing mechanisms for structural reliability and lifetime consumption (Marsh, 2016; Marsh et al., 2016; Pacheco et al., 2022; Pacheco, 2022). Accurate fatigue assessment is therefore central to certification, lifetime extension, and risk-informed asset management, particularly for ageing fleets operating under conditions that may deviate from design assumptions (IEC 61400-12-1, 2005; IEC 61400-13, 2015; Pacheco et al., 2022; Pacheco, 2022).

In practice, fatigue monitoring is commonly based on Supervisory Control and Data Acquisition (SCADA) data aggregated over conventional 10-minute windows (IEC 61400-13, 2015). These windows, aligned with long-established standards and certification procedures, typically provide statistical descriptors (means, standard deviations, extrema) of operational variables (IEC 61400-13, 2015). However, many fatigue-driving events occur on substantially shorter timescales, including rapid control adjustments, transient aerodynamic loading, and operational state changes (Marsh, 2016; Marsh et al., 2016; Pacheco et al., 2022; Pacheco, 2022). Aggregation over 10-minute windows may therefore smooth short-term stress fluctuations and distort the underlying cycle distribution, potentially biasing fatigue estimates (Marsh, 2016; Marsh et al., 2016).

Wind turbine manufacturers increasingly provide higher-frequency SCADA data at sub-minute intervals (Pacheco et al., 2022; Sadeghi et al., 2022, 2023). This development creates the opportunity to reassess fatigue monitoring strategies at shorter, SCADA-consistent timescales (Sadeghi et al., 2022, 2023). The objective is not to physically segment structural dynamics into artificial intervals, but to evaluate whether fatigue-relevant cycle information, especially large-amplitude cycles associated with slow variations in mean load and operational transitions, can be reliably preserved when stress data are aggregated at sub-minute resolution, enabling scalable monitoring without storing continuous high-frequency measurements. In this study, a 15-second window is adopted as the sub-minute aggregation interval, as this corresponds to the native temporal resolution at which the high-frequency SCADA data are available for the instrumented turbine.

Residual-preserving approaches, most notably the Low-Frequency Fatigue Dynamics (LFFD) methodology, address this limitation by extracting closed cycles within each window and reconstructing boundary-spanning cycles by concatenating residual stress sequences (Amzallag et al., 1994; Marsh, 2016; Marsh et al., 2016). Previous studies have demonstrated that this procedure preserves equivalence with continuous Rainflow Cycle Counting (RFC) while enabling window-based processing (Marsh, 2016; Marsh et al., 2016). However, existing applications have been formulated and validated almost

https://doi.org/10.5194/wes-2026-108
Preprint. Discussion started: 6 July 2026
© Author(s) 2026. CC BY 4.0 License.

eawe european academy of wind energy
Open Access WIND ENERGY SCIENCE DISCUSSIONS

exclusively within the conventional 10-minute windowing framework, and fatigue damage has typically been reported in aggregate form without explicit separation of cycle contributions arising within and across windows (Faria et al., 2024; Marsh, 2016; Marsh et al., 2016; Sadeghi et al., 2022, 2023).

In addition to residual-based approaches, reduced-information strategies based on extrema extraction have been proposed to reduce storage and computational demand requirements. By retaining only representative turning points per window (e.g. start–peaks–valleys–end or maximum–minimum values), these methods aim to preserve the sequence information required for Rainflow Cycle Counting (RFC) while substantially compressing the input signal (Larsen and Thomsen, 1996; Shah et al., 2025, 2026). Although extrema-based representations have been explored in the context of low-frequency fatigue effects, their performance has not been systematically benchmarked against residual-preserving methods using experimental tower strain data and sub-minute windows (Faria et al., 2024; Larsen and Thomsen, 1996; Sadeghi et al., 2022, 2023; Shah et al., 2025, 2026).

Previous experimental and simulation-based studies have shown that neglecting low-frequency fatigue dynamics can lead to a systematic underestimation of accumulated fatigue damage in wind turbine structures (Faria et al., 2024; Larsen and Thomsen, 1996; Marsh, 2016; Marsh et al., 2016; Sadeghi et al., 2022, 2023; Shah et al., 2025). Deviations reported between conventional 10-minute window based rainflow counting and approaches that preserve cycle continuity typically range from approximately 8% to more than 60%, depending on operating conditions, structural component, and fatigue curve formulation (Faria et al., 2024; Larsen and Thomsen, 1996; Marsh, 2016; Marsh et al., 2016; Sadeghi et al., 2022, 2023; Shah et al., 2025). A consistent trend across the literature is the strong dependence of this bias on the adopted Wöhler exponent m, as fatigue damage becomes increasingly dominated by relatively rare but large amplitude stress excursions associated with slow variations in mean load and operational transitions (Larsen and Thomsen, 1996; Sadeghi et al., 2022, 2023). For welded steel tower details represented by bi-linear $\sigma - N$ formulations with slopes $m = 3/5$, reported low-frequency contributions are typically on the order of 20–40% of total fatigue damage (Faria et al., 2024; Sadeghi et al., 2022, 2023), indicating that standard 10-minute windows may lead to materially non-conservative lifetime estimates. These findings highlight the need for fatigue monitoring strategies that preserve low-frequency cycle effects while remaining compatible with short, SCADA-aligned windows suitable for large-scale deployment (IEC 61400-13, 2015; Marsh, 2016; Marsh et al., 2016).

Despite the growing availability of high-frequency operational and structural data, three key gaps remain. First, the influence of reducing windows below 10 minutes on tower fatigue, as estimated from long-term field strain measurements, has not been comprehensively quantified. Second, although Low-Frequency Fatigue Dynamics (LFFD) has been applied in several studies, its capability to explicitly separate and characterise high- and low-frequency fatigue contributions (in the pragmatic monitoring sense adopted here), together with the associated cycle-count and damage spectra, has not been demonstrated using long-term wind turbine measurements, even within the conventional 10-minute framework. Third, the accuracy–storage trade-off of reduced-information extrema sequences has not been systematically evaluated relative to rainflow-equivalent residual-preserving methods using experimental data.

https://doi.org/10.5194/wes-2026-108
Preprint. Discussion started: 6 July 2026
© Author(s) 2026. CC BY 4.0 License.

eawe european academy of wind energy
Open Access WIND ENERGY SCIENCE DISCUSSIONS

To address these gaps, this study presents a comprehensive evaluation of fatigue monitoring methodologies using six months of high-frequency strain data from two instrumented tower sections of an onshore wind turbine. Continuous Rainflow Cycle Counting (RFC) is adopted as baseline and compared with (i) conventional window-based rainflow counting, (ii) a modified Low-Frequency Fatigue Dynamics (LFFD) implementation that explicitly separates intra-window (predominantly high-frequency) and inter-window (predominantly low-frequency) fatigue contributions through residual-sequence reconstruction, and (iii) reduced-information extrema sequence methods. The analysis investigates the influence of window length, sampling rate, and the selected $\sigma - N$ curve model used for damage calculation on accumulated damage, cycle spectra, and computational and storage requirements.

In this work, fatigue contributions are classified as high-frequency, corresponding to intra-window cycles (closing within a window), and low-frequency fatigue associated with inter-window cycles (spanning multiple windows and reconstructed through residual concatenation). This terminology is methodological and refers solely to signal segmentation; it does not represent a spectral decomposition of turbine loading processes. A physically high-frequency structural cycle may be categorised as inter-window if truncated by window boundaries.

The principal objective of this work is to enable fatigue assessment at a higher level of temporal granularity, extending beyond cumulative damage estimation alone. Here, granularity refers to both the temporal discretisation of the stress signal and the explicit separation of fatigue contributions into intra-window and inter-window components. By resolving these contributions across different window lengths and analysing the associated cycle-count and damage spectra, the study provides (i) a quantitative benchmark of window- and sampling-driven deviations relative to continuous rainflow counting, (ii) a structured decomposition of fatigue into high-frequency (intra-window) and low-frequency (inter-window) fatigue contributions, and (iii) an accuracy–storage–computation comparison of residual-preserving and extrema-based representations. Together, these results establish a practical basis for SCADA-aligned, data-efficient fatigue monitoring suitable for wind-farm-scale deployment and lifetime extension applications.

A preliminary version of part of this analysis, restricted to one month of data and to the high-/low-frequency LFFD partitioning with simple value-sequence representations, was presented at the TORQUE conference (Oliveira et al., 2026). The present work substantially extends it through a six-month dataset, the continuous rainflow baseline, the Max–Min representation, the EC3–DNV comparison, and the accuracy–storage–computation benchmark.

This paper is structured as follows. Section 2 presents the fatigue-damage estimation methodologies considered in this study, including continuous Rainflow Cycle Counting (RFC) as baseline, window-based approaches, the residual-preserving Low-Frequency Fatigue Dynamics (LFFD) framework, and reduced-information extrema-sequence methods, together with the metrics used for quantitative comparison. Section 3 introduces the experimental dataset and case study, describing the instrumented wind turbine, the measurement campaign, and the signal pre-processing steps. Section 4 presents and discusses the experimental results, analysing the influence of sampling rate and fatigue-curve formulation on cumulative damage, the effect of window length on fatigue partitioning, and a systematic comparison of all monitoring methods

https://doi.org/10.5194/wes-2026-108
Preprint. Discussion started: 6 July 2026
© Author(s) 2026. CC BY 4.0 License.

in terms of accuracy, data storage, and computational requirements. Finally, Section 5 summarises the main findings and discusses their implications for scalable, SCADA-aligned fatigue monitoring and lifetime assessment of wind turbine towers.

2 Fatigue Damage Estimation Methodologies

2.1 Continuous Rainflow Cycle Counting (Baseline Counting Method)

When continuous strain measurements are available, fatigue assessment can be performed by applying Rainflow Cycle Counting (RFC) directly to the full, unsegmented stress time series (Amzallag et al., 1994; Matsuishi and Endo, 1968; McInnes and Meehan, 2008). By preserving the complete sequence of stress reversals, this approach provides the most accurate reconstruction of the fatigue spectrum, including both full and half cycles (Figure 1a-b).

In this work, continuous Rainflow Cycle Counting (RFC) applied to the full stress history is adopted as the baseline fatigue assessment against which all alternative methodologies are benchmarked. Although computationally demanding and therefore impractical for long-term operational monitoring at scale, it provides a consistent and objective baseline for quantifying the effect of signal window length, residual processing, and information reduction (Marsh, 2016; Marsh et al., 2016).

2.2 Window-based High-cycle Counting

In practice, fatigue assessment of wind turbine towers is commonly based on fixed-duration windowing, typically using 10-minute windows in accordance with IEC 61400-13 (IEC 61400-13, 2015). In this approach, the stress time series is segmented into consecutive windows of equal duration (Figure 1c), and Rainflow Cycle Counting (RFC) is applied independently to each window (Figure 1d). Cycle counts, including full and half cycles, are then aggregated across windows to obtain cumulative fatigue damage (Figure 1e).

While widely adopted, window-based high-cycle counting exhibits an inherent limitation: stress excursions that span multiple windows are truncated at window boundaries. This truncation leads to the loss of large-amplitude, long-period cycles associated with slowly varying mean stresses, resulting in non-conservative fatigue life estimates when such cycles contribute significantly to damage (Marsh, 2016; Marsh et al., 2016).

https://doi.org/10.5194/wes-2026-108
Preprint. Discussion started: 6 July 2026
© Author(s) 2026. CC BY 4.0 License.

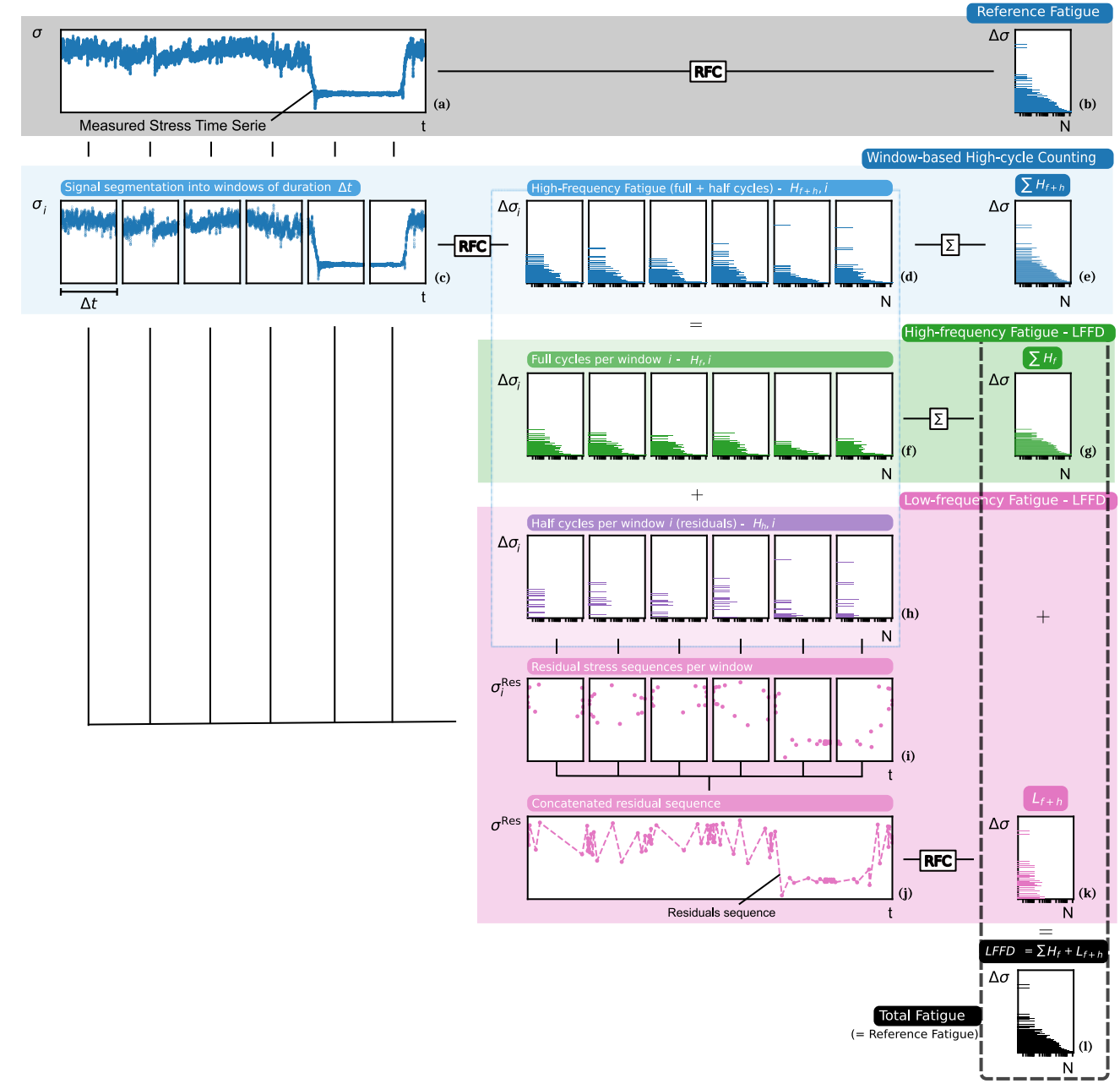

Figure 1. Overview of fatigue monitoring methodologies based on Rainflow Cycle Counting (RFC). (a) Measured stress time series. (b) Baseline fatigue spectrum obtained by applying RFC to the full signal, including full and half cycles. (c) Segmentation of the stress time series into consecutive windows of duration Δt. (d) RFC applied independently to each window, yielding window-level fatigue spectra. (e) Aggregated fatigue spectrum obtained by summing full and half cycles across all windows. (f) Full cycles extracted within each window. (g) Aggregated full-cycle spectrum representing the high-frequency, window-contained fatigue contribution. (h) Half cycles remaining in each window. (i) Residual stress sequences associated with unclosed half cycles. (j) Concatenation of residual stress sequences across windows. (k) RFC applied to the concatenated residual sequence, capturing low-frequency fatigue cycles spanning multiple windows. (l) Total fatigue spectrum obtained by combining the high-frequency (full-cycle) and low-frequency (residual-based) contributions, preserving equivalence with continuous RFC.

https://doi.org/10.5194/wes-2026-108
Preprint. Discussion started: 6 July 2026
© Author(s) 2026. CC BY 4.0 License.

eawe european academy of wind energy
Open Access WIND ENERGY SCIENCE DISCUSSIONS

2.3 Low-Frequency Fatigue Dynamics (LFFD)

Residual-preserving fatigue analysis originates from the formalisation of rainflow cycle counting (Amzallag et al., 1994), which introduced the residual sequence to represent unclosed stress excursions after cycle extraction. The importance of long-period loading effects in wind turbine fatigue was subsequently highlighted by Larsen and Thomsen, who showed that large-amplitude cycles associated with operational transitions can disproportionately contribute to fatigue damage, particularly for higher Wöhler exponents (Larsen and Thomsen, 1996). To avoid artificial cycle closure and double counting inherent to conventional window-based approaches, Marsh et al. demonstrated that extracting closed cycles within each window and concatenating the remaining residual sequences preserves equivalence with continuous rainflow counting (Marsh, 2016; Marsh et al., 2016). This residual-preserving framework, later termed Low-Frequency Fatigue Dynamics (LFFD), has since been validated using long-term wind turbine strain measurements and shown to capture fatigue contributions that are otherwise systematically underestimated (Faria et al., 2024; Sadeghi et al., 2022, 2023; Shah et al., 2025, 2026).

Within this framework, Rainflow Cycle Counting (RFC) is first applied independently to each window to extract closed cycles (Figure 1f). The remaining unclosed stress excursions are retained as residual stress sequences (Figure 1h–i), which are concatenated across windows (Figure 1j) and subsequently processed using Rainflow Cycle Counting (RFC) to recover cycles spanning multiple windows (Figure 1k). The resulting fatigue response can be expressed as the sum of two contributions: a high-frequency contribution associated with cycles fully contained within individual windows, and a low-frequency contribution associated with cycles reconstructed from the concatenated residual sequence. Their combination is equivalent to the fatigue spectrum obtained using continuous Rainflow Cycle Counting (RFC) (Figure 1l), thereby preserving rainflow equivalence (Marsh, 2016; Marsh et al., 2016).

In this study, a modified Low-Frequency Fatigue Dynamics (LFFD) implementation is adopted to explicitly quantify high and low-frequency fatigue contributions while maintaining equivalence with the baseline method (Figure 2). This explicit separation enables a more granular characterisation of fatigue behaviour and is particularly relevant when the window length is reduced below the conventional 10-minute duration.

https://doi.org/10.5194/wes-2026-108
Preprint. Discussion started: 6 July 2026
© Author(s) 2026. CC BY 4.0 License.

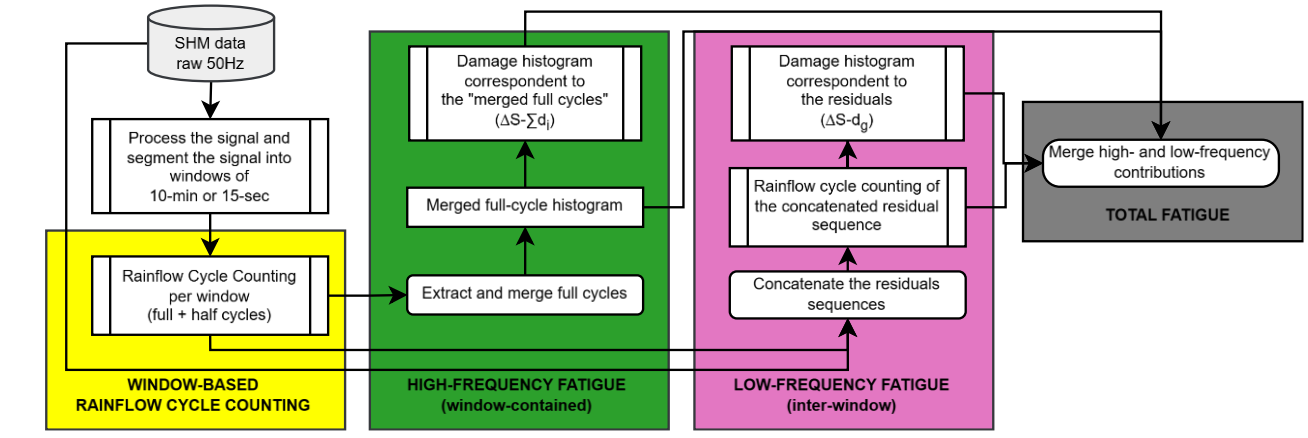

Figure 2. Simplified flowchart of the modified Low-Frequency Fatigue Dynamics (LFFD) methodology, inspired in (Faria et al., 2024; Sadeghi et al., 2022). Following signal pre-processing and windowing, Rainflow Cycle Counting (RFC) is applied independently within each window. High-frequency fatigue (green) is obtained from merged full-cycle histograms, while low-frequency fatigue (pink) is derived from RFC applied to concatenated residual sequences across windows. Damage and cycle-count histograms are computed separately for each contribution and subsequently merged to obtain the total fatigue response (grey), preserving equivalence with continuous rainflow counting.

2.4 Extrema Sequence Methods

Rainflow counting is inherently sequence dependent, relying solely on the order and magnitude of stress turning points (Amzallag et al., 1994; Matsuishi and Endo, 1968; McInnes and Meehan, 2008). This property motivates reduced information fatigue representations in which the full stress time series is replaced by a simplified sequence of representative extrema, substantially reducing data volume and computational effort.

Two extrema-based representations are considered in this work (Figure 3). The Start–Peaks–Valleys–End (SPVE) approach retains, for each window, the start, peaks, valleys, and end values of the stress signal (Figure 3b). Concatenation of these points forms a continuous extrema sequence (Figure 3c), to which Rainflow Cycle Counting (RFC) is applied once to identify fatigue cycles, including those spanning multiple windows (Figure 3d).

A further reduction is achieved using the Maximum–Minimum (Max–Min) approach, which retains only the maximum and minimum stress values within each window (Figure 3e–f). This representation emphasises large-amplitude, long-period stress variations associated with operational transitions and enables extreme data compression with minimal computational cost (Larsen and Thomsen, 1996; Shah et al., 2025, 2026).

Extrema sequence methods are examined here as reduced information representations that complement, rather than replace, residual-preserving approaches. Their performance is evaluated relative to continuous Rainflow Cycle Counting (RFC) and Low-Frequency Fatigue Dynamics (LFFD) in terms of fatigue accuracy, window length, and data handling efficiency.

https://doi.org/10.5194/wes-2026-108
Preprint. Discussion started: 6 July 2026
© Author(s) 2026. CC BY 4.0 License.

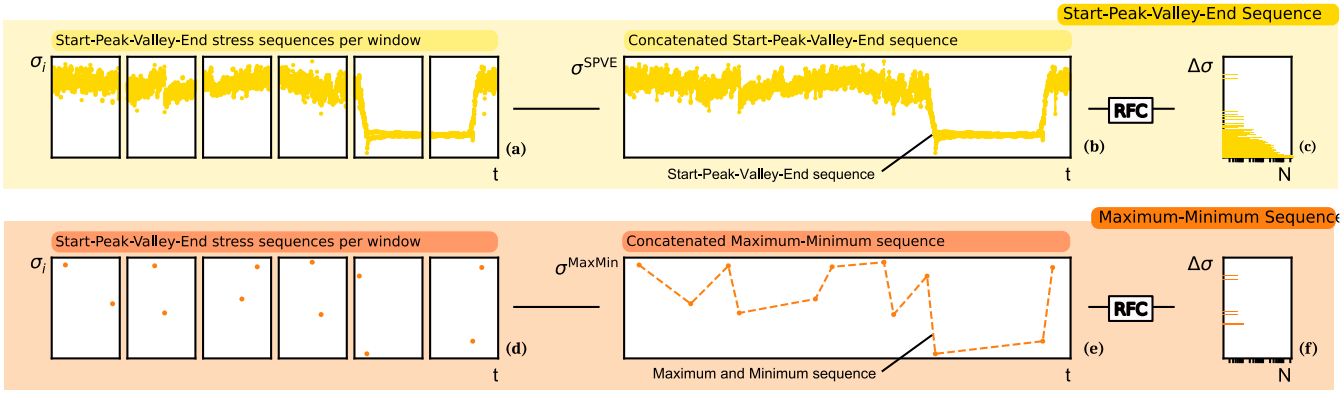

Figure 3. Extrema sequence methods for reduced-information fatigue assessment. (a) Measured stress time series segmented into windows of duration Δt. (b) Windowed extraction of start, peaks, valleys, and end (SPVE) points within each window. (c) Concatenation of the windowed SPVE values to form a continuous start-peaks–valleys–end sequence. (d) Fatigue spectrum obtained by applying RFC to the concatenated SPVE sequence. (e) Windowed extraction of global maximum and minimum stress values. (f) Concatenation of windowed maxima and minima to form a maximum–minimum (Max-Min) sequence. (g) Rainflow Cycle Counting (RFC) applied to the Max-Min sequence. (h) Corresponding fatigue spectrum derived from the Max-Min representation. The SPVE approach preserves local turning-point structure, while the Max-Min approach provides a highly compressed representation emphasising large-amplitude, long-period stress variations.

2.5 Metrics for Fatigue Evaluation

To establish a consistent and quantitative comparison between fatigue assessment methodologies for wind turbine towers, this study evaluates performance based on five complementary dimensions: (i) the relative contribution of low- and high-frequency fatigue damage components, (ii) sensitivity of fatigue damage estimates to the adopted design standard, (iii) sensitivity to signal temporal resolution (sampling rate and window length), (iv) agreement of alternative monitoring methodologies with a baseline fatigue assessment, and (v) data reduction quantification.

Fatigue assessment in the present work is based on the evaluation of accumulated fatigue damage, under the assumption of linear damage accumulation with the number of applied load cycles at each stress level (Pacheco et al., 2022; Pacheco, 2022). Accordingly, the Palmgren–Miner linear damage accumulation rule (Kauzlarich, 1989; Miner, 1945) is adopted, whereby the total fatigue damage is obtained by summing the individual damage contributions associated with all stress ranges over the entire time series:

$$\boldsymbol{D} = \sum_{i=1}^{n_\sigma} \frac{n_i}{N_i} \tag{1}$$

where i denotes the $i-th$ stress range bin, n_i is the number of cycles counted at the stress range σ_i, and N_i is the corresponding number of cycles to failure.

Two $\sigma - N$ curve formulations are considered: EC3 (Eurocode 3) detail category 80 and DNVGL-RP-C203 welded-steel, both using a bi-linear $\sigma - N$ curve with slopes $m = 3/5$.

https://doi.org/10.5194/wes-2026-108
Preprint. Discussion started: 6 July 2026
© Author(s) 2026. CC BY 4.0 License.

eawe european academy of wind energy
Open Access WIND ENERGY SCIENCE DISCUSSIONS

The specific metrics adopted in this work and their mathematical definitions are summarised in Table 1, which provides a structured overview of the performance indicators used throughout the analysis together with the associated equation numbers. These metrics are applied consistently in the following sections to enable objective comparisons across monitoring methodologies, temporal resolutions, and modelling assumptions.

Table 1. Overview of fatigue damage metrics adopted in the present study.

Objective	Equation	Equation Number
Quantification of the relative contribution of low- and high-frequency fatigue damage components within the LFFD framework	$D_{i,total}\ [\%] = \frac{D_{LFFD,i}}{D_{LFFD,total}} \times 100$	(2)
Comparison of fatigue damage obtained using different design standards (EC3 vs. DNV $\sigma - N$ curves)	$D_{EC3,DNV}\ [\%] = \left(\frac{D_{DNV} - D_{EC3}}{D_{DNV}}\right) \times 100$	(3)
Assessment of the influence of signal sampling rate on fatigue damage estimation	$D_{freq,50Hz}\ [\%] = -\left(\frac{D_{50Hz} - D_{freq}}{D_{50Hz}}\right) \times 100$	(4)
Performance comparison of fatigue monitoring methodologies relative to the baseline fatigue assessment	$Damage\ ratio\ /\ D^{EC3}_{method}[\%] = \frac{D_{method}}{D_{Ref}} \times 100$	(5)
Data reduction relative to the raw data length	$Data\ reduction\ [\%] = \left(\frac{N_{raw} - N_{method}}{N_{raw}}\right) \times 100$	(6)

where:

- $D_{i,total}$ is the percentage contribution of component i to the total fatigue damage.
- $D_{LFFD,i}$, with $i \in \{low, high\}$, is the fatigue damage of component i relative to the total damage $D_{LFFD,total}$ obtained by the LFFD methodology.
- D_{DNV} is the fatigue damage computed using DNVGL-RP-C203 curve.
- D_{EC3} is the fatigue damage computed using EC3 curve, category 80.
- D_{50Hz} is the fatigue damage computed from the baseline signal sampled at 50 Hz.
- D_{freq} is the fatigue damage computed from the signal decimated with the data sampling rate $freq$, with $freq = \{6.25, 12.5, 25\}\ [Hz]$.
- D^{EC3}_{method} is the fatigue damage estimated for each method under evaluation, with $method = \{L_{f+h}, SPVE, Max - Min, H_{f+h}\}$
- D_{Ref} is the baseline fatigue damage estimated considering a continuous Rainflow Cycle Counting (RFC) of the signal, without segmentation.
- N_{raw} is the number of points that belong to the raw signal.
- N_{method} is the number of the points that belong to the sequence signal for each method, with $method = \{L_{f+h}, SPVE, Max - Min\}$.

3 Case Study and Experimental Data

The dataset used in this study combines SCADA operational and environmental data with measurements from a Structural Health Monitoring (SHM) system installed on a multi-megawatt onshore wind turbine with an 80 m rotor diameter. The SHM system instruments two tower sections, T1 and T2, located approximately 54 m and 71 m above ground level, respectively (Figure 4a). Each section is equipped with four circumferential resistive strain gauges (S1–S4) and one PT100 temperature sensor (Figure 4b–c). Although accelerometers are also available, they are not considered in the present work. All SHM channels were sampled at 50 Hz.

https://doi.org/10.5194/wes-2026-108
Preprint. Discussion started: 6 July 2026
© Author(s) 2026. CC BY 4.0 License.

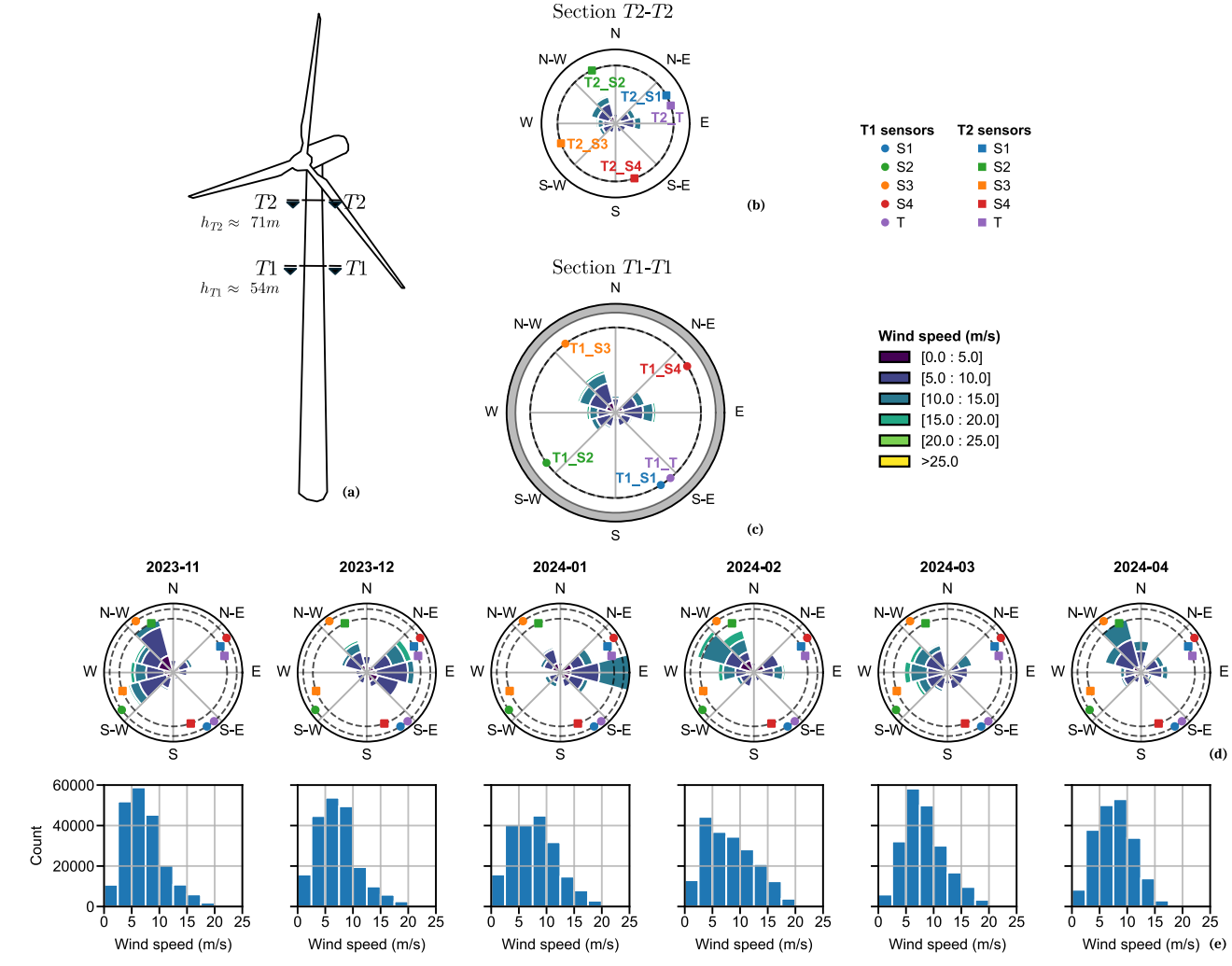

Figure 4. Turbine instrumentation and inflow conditions. (a) Instrumented tower sections T1 and T2. (b–c) Sensor layout at each section (strain gauges S1–S4 and temperature sensor T). (d) Monthly wind roses and (e) wind speed histograms for Nov 2023–Apr 2024.

https://doi.org/10.5194/wes-2026-108
Preprint. Discussion started: 6 July 2026
© Author(s) 2026. CC BY 4.0 License.

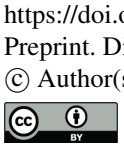

eawe european academy of wind energy
Open Access WIND ENERGY SCIENCE DISCUSSIONS

Figure 5 summarises the wind turbine's operational behaviour during the analysed period and provides context for the strain-based fatigue assessment. Figure 5a–d present the relationships between power, pitch angle, generator speed, rotor speed, and wind speed. The data points are coloured according to the turbine operational status, including Run, Ready, STOP, Ambient Cable Unwind, and other less frequent states.

The dataset is dominated by normal turbine operation, with the Run state accounting for 87.24% of all samples. The Ready state accounts for an additional 11.49%, while the remaining operational states correspond to only a small fraction of the dataset. This distribution confirms that the analysed period is primarily characterised by standard power-production conditions, with relatively limited occurrence of shutdown or transient operational events.

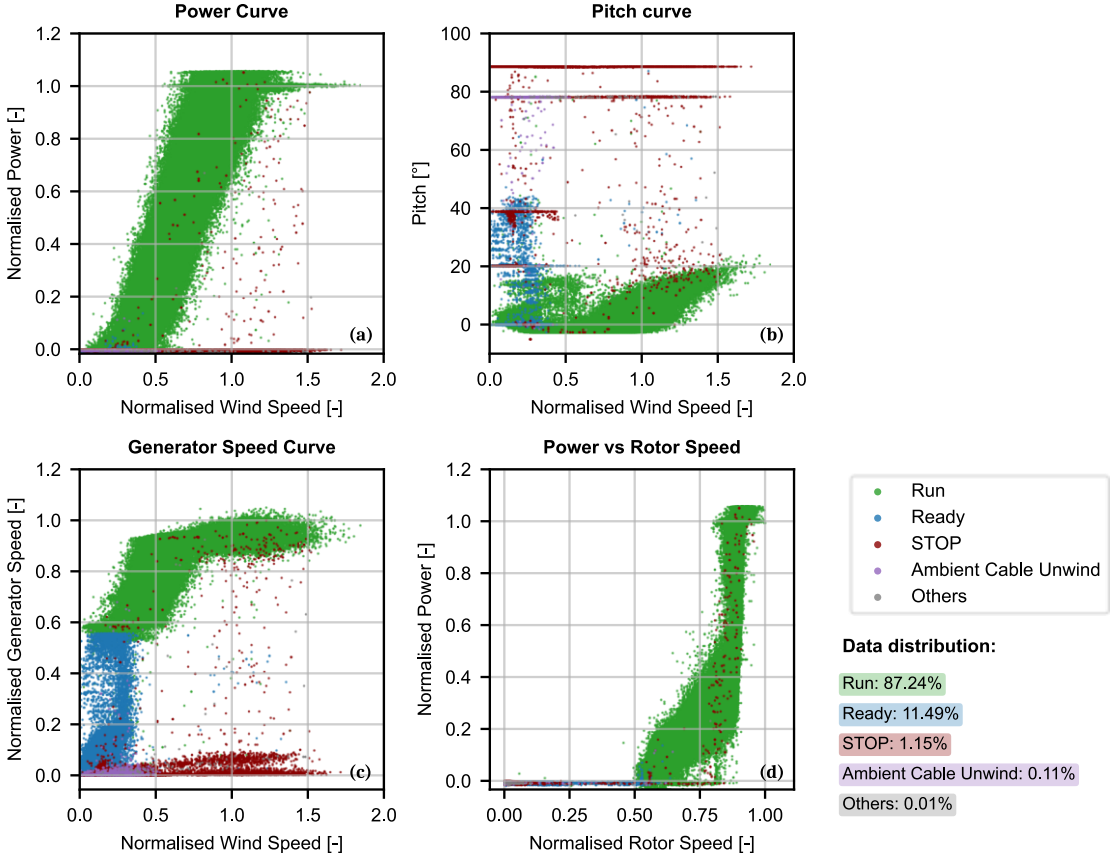

Figure 5. SCADA operational curves for the study period (15-second data). (a-c) Normalised power, pitch, and generator-speed curves versus normalised wind speed. (d) Normalised power versus normalised rotor speed. Colours indicate operational status; the right panel shows the sample distribution by status.

https://doi.org/10.5194/wes-2026-108
Preprint. Discussion started: 6 July 2026
© Author(s) 2026. CC BY 4.0 License.

eawe european academy of wind energy
Open Access WIND ENERGY SCIENCE DISCUSSIONS

4 Analysis of Experimental Data

4.1 Stress-damage ($\Delta\sigma - D$) Representations

Fatigue results are commonly represented using stress–cycle ($\Delta\sigma - N$) distributions. In the present work, stress–damage ($\Delta\sigma - D$) distributions are additionally employed to highlight the stress ranges that dominate fatigue damage accumulation explicitly.

Figure 6 compares different $\Delta\sigma - N$ and $\Delta\sigma - D$ representations for 10-minute windows as an example. Figure 6a–c uses logarithmic scaling on the y-axis, while Figure 6d–f uses linear scaling on the y-axis. Figure 6a and Figure 6d show the corresponding $\Delta\sigma - N$ histograms together with the reference EC3 and DNV $\sigma - N$ curves. Figure 6b and Figure 6e present the associated $\Delta\sigma - D$ distributions using logarithmic scaling on the x-axis, whereas Figure 6c and Figure 6f show the same $\Delta\sigma - D$ distributions using linear scaling on the x-axis. In all cases, the fatigue contributions are decomposed into high-frequency (green) and low-frequency (pink) Low-Frequency Fatigue Dynamics (LFFD) components, while the black curve represents the total fatigue distribution.

The comparison highlights how the choice of axis scaling influences the apparent smoothness of the fatigue distributions and the visibility of the damage-dominant stress ranges. Logarithmic scaling produces smoother $\Delta\sigma - D$ curves and can facilitate trend identification across a broad range of stress intervals. However, it may also reduce the visibility of the relative contribution of individual stress ranges to the overall fatigue damage. In contrast, linear scaling provides a clearer representation of where damage accumulates within the spectrum and improves the identification of the dominant fatigue ranges. For this reason, the remainder of the analysis adopts linear scaling for both axes in the $\Delta\sigma - D$ representations.

https://doi.org/10.5194/wes-2026-108
Preprint. Discussion started: 6 July 2026
© Author(s) 2026. CC BY 4.0 License.

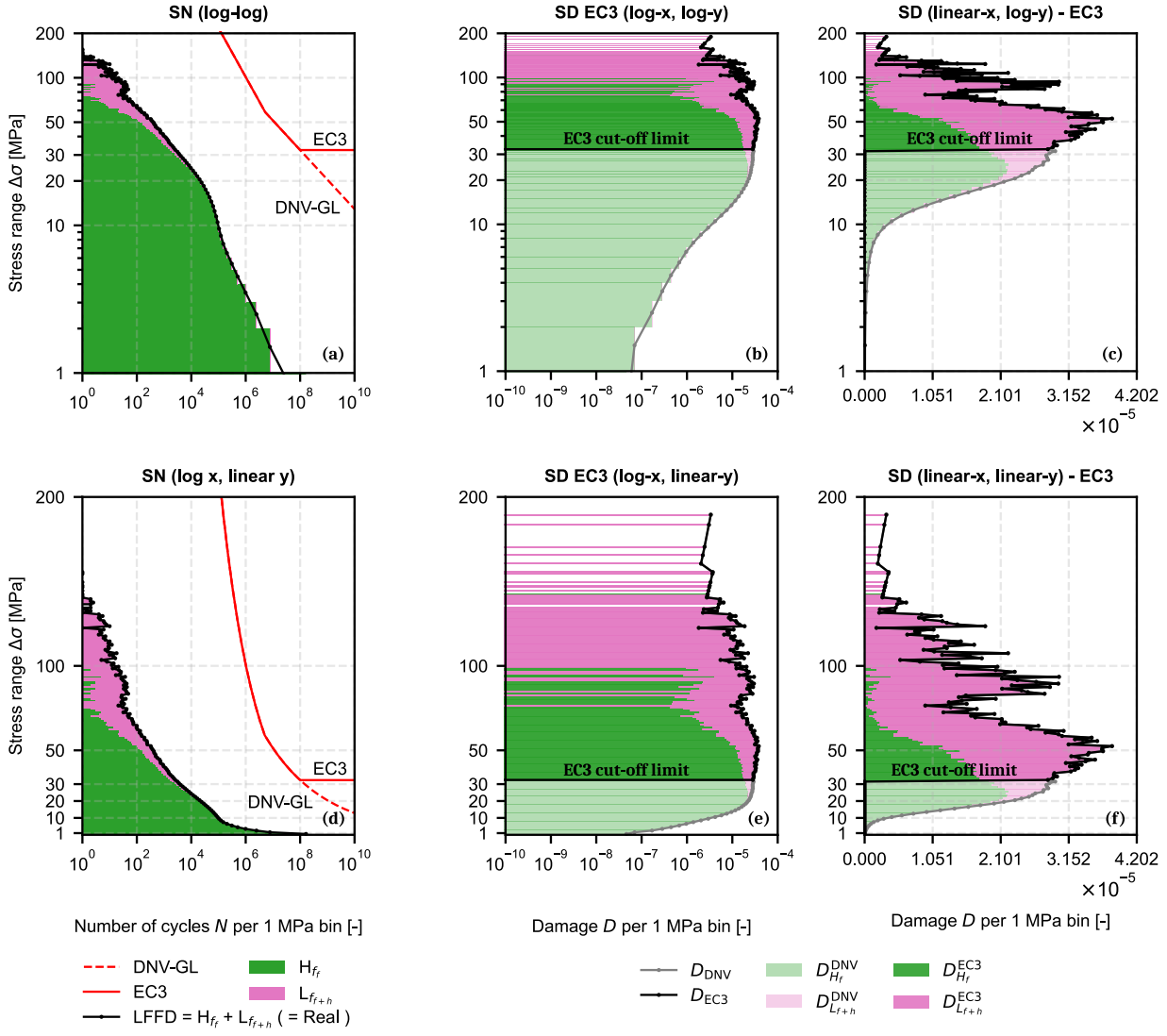

Figure 6. Comparison of $\Delta\boldsymbol{\sigma} - \boldsymbol{N}$ and $\Delta\boldsymbol{\sigma} - \boldsymbol{D}$ fatigue representations for conventional 10-minute windows. Panels (a) and (d) show the $\Delta\boldsymbol{\sigma} - \boldsymbol{N}$ distributions together with the EC3 and DNV $\boldsymbol{\sigma} - \boldsymbol{N}$ curves. The top row (a–c) uses logarithmic scaling on the y-axis, while the bottom row (d–f) uses linear scaling on the y-axis. Panels (b) and (e) present the corresponding $\Delta\boldsymbol{\sigma} - \boldsymbol{D}$ distributions with logarithmic scaling on the x-axis, whereas panels (c) and (f) show the same distributions using linear scaling on the x-axis. Green and pink denote the LFFD high-frequency and low-frequency fatigue contributions, respectively, while the black curve represents the total fatigue distribution.

4.2 Assessment of Standards in Damage Calculation

Eurocode 3 (EC3) provides fatigue classes explicitly linked to welded steel details typical of tubular towers, such as longitudinal and circumferential welds and attachments, enabling detail-specific fatigue assessment. In contrast, the DNVGL-RP-C203 (DNV) defines broader welded-steel fatigue classes developed for a wider range of offshore and onshore applications, which can result in different levels of conservatism when applied to tower shell structures. For lifetime-extension assessments, the choice of fatigue standard can therefore materially influence the inferred remaining life.

https://doi.org/10.5194/wes-2026-108
Preprint. Discussion started: 6 July 2026
© Author(s) 2026. CC BY 4.0 License.

Figure 7 compares the relative differences between EC3- and DNV-based fatigue damage estimates for 10-minute and 15-second windows, considering both total fatigue damage and its low- and high-frequency contributions. Damage was computed using EC3 (Eurocode 3) detail category 80 and DNVGL-RP-C203 welded-steel, both using a bi-linear $\sigma - N$ curve with slopes $m = 3/5$. Because Low-Frequency Fatigue Dynamics (LFFD) preserves the total accumulated fatigue damage across windows, the relative difference between EC3- and DNV-based total damage estimates is unaffected by window length. However, changes in window length alter the partitioning between low- and high-frequency contributions, thereby altering how each fatigue standard weights the underlying stress-range distribution. For tower section T1 in the fore-aft direction, EC3 yields fatigue-damage estimates that are 17.4% lower than those obtained using DNV for both window lengths (Figure 7c). The reduction increases to 66.1% at section T2, consistent with a stress-range distribution dominated by lower-amplitude cycles at higher elevations, which are weighted differently by the EC3 and DNV $\sigma - N$ formulations. Comparable trends are observed in the side-to-side (SS) direction at both tower sections (Figure 7b and Figure 7d).

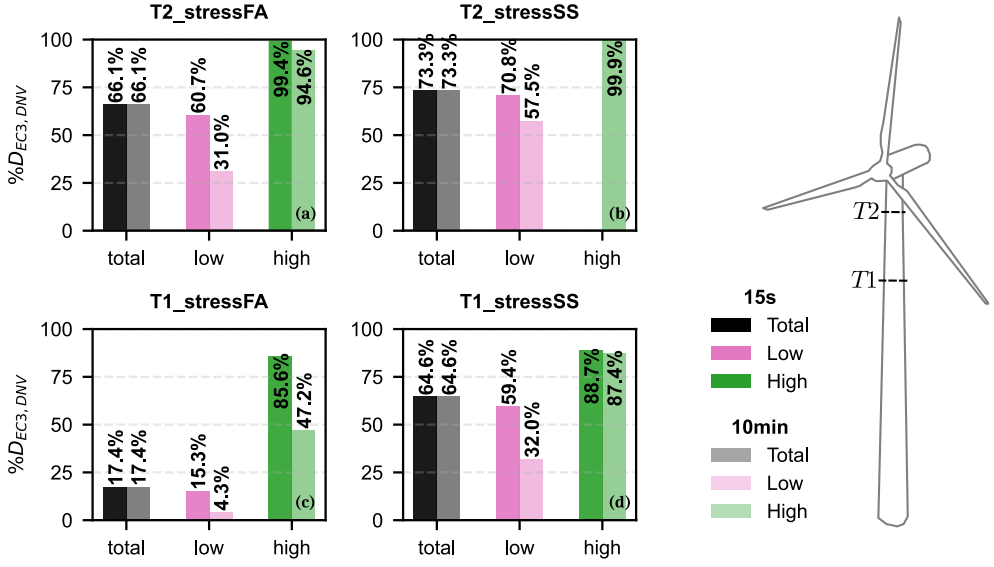

Figure 7. Relative differences between fatigue damage estimates obtained using Eurocode 3 (EC3) and DNVGL-RP-C203 (DNV) for 10-minute and 15-second windows. Damage is computed using EC3 detail category 80 and DNVGL-RP-C203 welded-steel $\boldsymbol{\sigma - N}$ curves, both employing a bi-linear formulation with slopes $\boldsymbol{m = 3/5}$. Results are shown for tower section T1 (near-base) and T2 (upper tower) in the fore–aft (FA) and side-to-side (SS) directions: (a) T2–FA, (b) T2–SS, (c) T1–FA, (d) T1–SS. Bars indicate percentage differences in accumulated damage between EC3 and DNV for the total fatigue damage and for the low- and high-frequency contributions, computed using Equation (3).

4.3 Influence of the Data Sampling Rate

In the previously presented analysis, results were shown for data sampled at 50 Hz, which corresponds to the acquisition frequency of the strain measurements. Although high-frequency data are desirable for fatigue evaluation, processing long-term measurements at such high sampling rates is computationally impractical. For this reason, the 50 Hz strain signals were decimated to 25, 12.5, and 6.25 Hz. The minimum rate (6.25 Hz) was selected to remain above the dominant structural-

https://doi.org/10.5194/wes-2026-108
Preprint. Discussion started: 6 July 2026
© Author(s) 2026. CC BY 4.0 License.

response bandwidth observed in the measurements (most energy below ~5 Hz). The baseline damage for sampling-rate comparisons is defined as the 50 Hz continuous rainflow result.

Sampling-rate effects were assessed for (i) the total accumulated damage and for (ii) the low- and high-frequency contributions. Because total Low-Frequency Fatigue Dynamics (LFFD) damage is rainflow-equivalent, any change due to decimation reflects a loss of cycle resolution rather than windowing effects; changes in the low-frequency and high-frequency partitions are interpreted in the context of the selected window length.

Figure 8 shows cumulative damage at tower section T1 direction Fore-Aft (FA) for four sampling rates (50, 25, 12.5, and 6.25 Hz) and two window lengths (10-minute and 15-second). Total damage and its low-frequency and high-frequency components are reported using the EC3 model, and end-of-period values are annotated with deviations relative to the 50 Hz baseline.

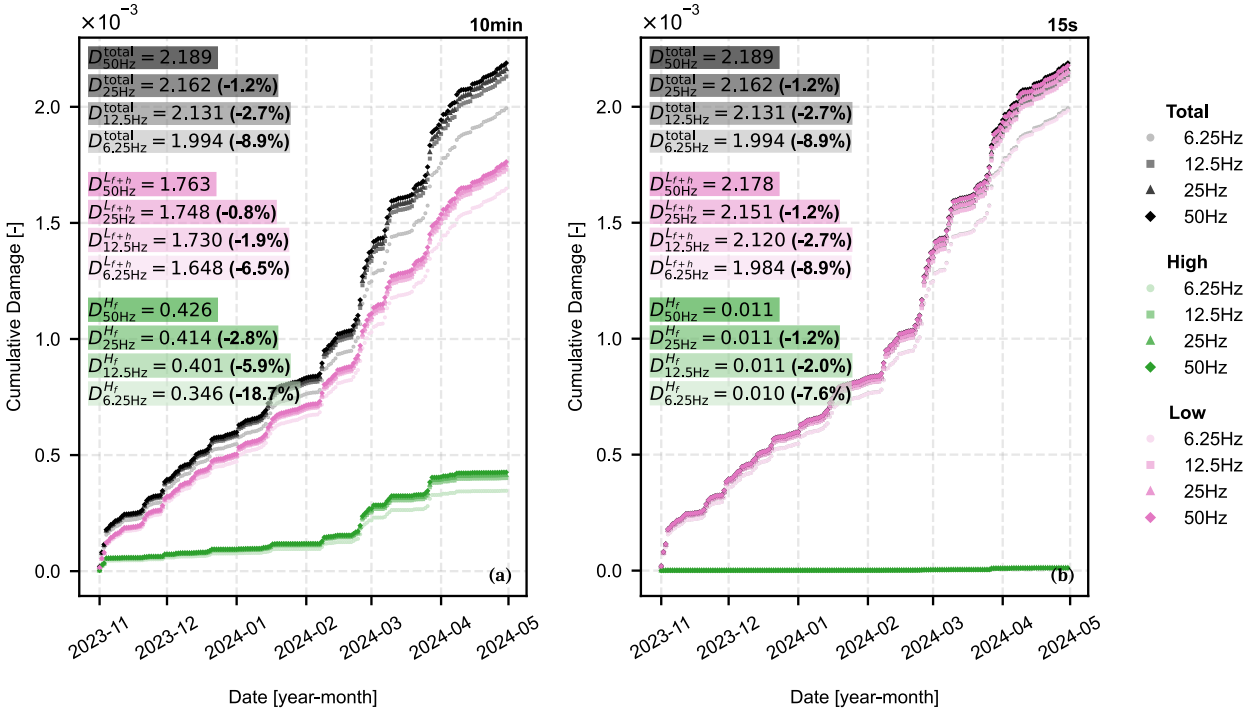

Figure 8. Cumulative FA-direction damage at tower section T1 for four sampling rates and two window lengths: (a) 10-minute and (b) 15-second. Curves show total, low-frequency, and high-frequency contributions computed with EC3 detail category 80 curve; annotations report end-of-period values and deviations from the 50 Hz baseline, computed by Equation (4).

Total accumulated damage decreases systematically with sampling rate, with reductions up to ~9% at 6.25 Hz relative to 50 Hz (Figure 8). The close agreement at 25 Hz and 12.5 Hz (reductions of ~1.2% and ~3%, respectively) indicates that these rates capture most fatigue-relevant content in this signal. At 6.25 Hz, damage is modestly underestimated but remains within ~9%.

https://doi.org/10.5194/wes-2026-108
Preprint. Discussion started: 6 July 2026
© Author(s) 2026. CC BY 4.0 License.

eawe european academy of wind energy
Open Access WIND ENERGY SCIENCE DISCUSSIONS

Low-frequency damage is relatively robust to decimation. For 10-minute windows, reductions remain <1% at 25 Hz and increase to ~6.5% at 6.25 Hz; similar behaviour occurs for 15-second windows, with differences mainly in the low- and high-frequency partitions rather than in total damage.

High-frequency damage is more sensitive to decimation. For 10-minute windows, high-frequency damage decreases substantially with sampling rate, reaching ~20% reduction at 6.25 Hz. For 15-second windows, within-window closed-cycle damage is already small because most excursions do not close within a short window; decimation further reduces the remaining within-window cycle resolution.

Figure 9 summarises the relative damage loss with respect to 50 Hz for Fore-Aft (FA) and Side-to-Side (SS) at tower section T1, for total damage and the low-frequency and high-frequency components, and for both 10-minute and 15-second windows. Values are shown as six-month means with standard deviations.

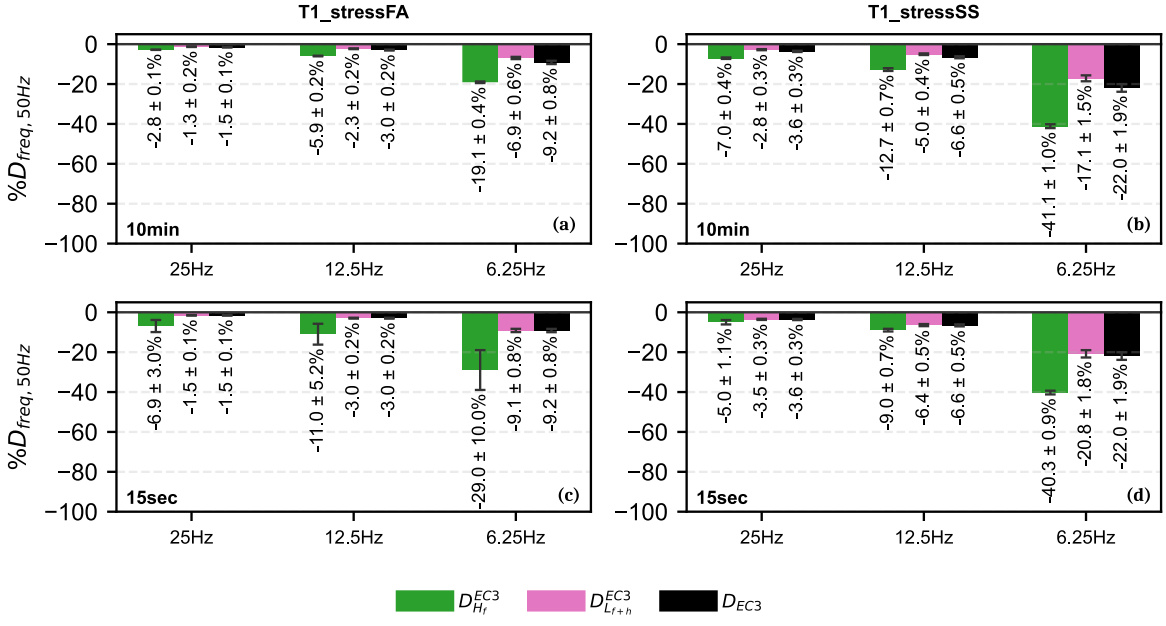

Figure 9. Relative damage loss with respect to 50 Hz at tower section T1 for Fore-Aft (FA) and Side-to-Side (SS), computed by Equation (4). Bars show total, low-frequency, and high-frequency contributions for 25, 12.5, and 6.25 Hz, using 10-minute and 15-second windows. Values are six-month means with standard deviations. Damage computed with EC3 detail category 80 curve.

Across both directions and window lengths, total damage loss increases as sampling rate decreases (Figure 9). At 25 Hz and 12.5 Hz, total losses are typically below ~3.6%, while at 6.25 Hz losses increase to ~9% in Fore-Aft (FA) and exceed ~20% in Side-to-Side (SS), indicating higher sensitivity of the SS response to undersampling.

The low-frequency component shows moderate and consistent sensitivity, remaining below ~10% loss in Fore-Aft (FA) and below ~21% in Side-to-Side (SS) at 6.25 Hz. In contrast, the high-frequency component is substantially more sensitive, particularly for 10-minute windows, where losses can reach ~20–40% at 6.25 Hz depending on direction.

https://doi.org/10.5194/wes-2026-108
Preprint. Discussion started: 6 July 2026
© Author(s) 2026. CC BY 4.0 License.

Although sampling rates of 25 Hz and 12.5 Hz provide closer agreement with the 50 Hz baseline, the 6.25 Hz case is retained in the subsequent analysis as a deliberately conservative lower-resolution scenario. The objective is not to identify an optimal sampling rate, but to evaluate the robustness of the proposed fatigue-monitoring strategies under restrictive temporal resolution and computational constraints. The use of 6.25 Hz, therefore, represents a lower-bound scenario in which the resulting bias in total fatigue damage remains bounded and explicitly quantified for the present dataset. While the magnitude of this bias is inherently case-dependent and may vary across turbine configurations and response characteristics, adopting the lowest admissible sampling rate provides a stringent, transparent basis for benchmarking reduced-information fatigue-monitoring approaches under realistic large-scale deployment conditions.

4.4 Influence of Window Length

To isolate the influence of window length on fatigue characterisation without conflating it with information loss, the analysis first considers window-length effects within the residual-preserving Low-Frequency Fatigue Dynamics (LFFD) framework. This enables assessment of the effect of window segmentation itself, before introducing additional approximations associated with reduced-information representations.

The selection of the window directly influences how stress excursions are classified between within-window full cycles and residual-based cycles spanning adjacent windows in the Low-Frequency Fatigue Dynamics (LFFD). Reducing the window length increases the likelihood that slowly varying stress excursions remain unclosed within an individual window and are therefore transferred to the residual sequence. Consequently, although the total fatigue damage remains theoretically equivalent to continuous rainflow counting, the relative contribution of the identified high- and low-frequency fatigue components may change significantly with the adopted window duration.

Figure 10 presents the fatigue response in the Fore–Aft (FA) direction at tower section T1, which exhibits the highest accumulated fatigue damage. Results are shown for 50 Hz strain data aggregated using 10-minute and 15-second windows. Panels (a–b) show cumulative damage, and panels (c–d) show the final $\Delta\sigma - D$ spectra. Total damage (black/grey) is decomposed into within-window high-frequency full-cycle damage (green) and low-frequency full- and half-cycle damage spanning windows (pink) and is computed using both EC3 and DNV.

As shown in Figure 10, the total fatigue damage obtained with Low-Frequency Fatigue Dynamics (LFFD) is independent of window length, because the method preserves rainflow equivalence through the combination of within-window full cycles and the concatenated residual sequence. The absolute damage level depends on the adopted $\boldsymbol{\sigma - N}$ curve; this effect is discussed in Section 4.2. In contrast to the total damage, the partition between low- and high-frequency contributions changes markedly with window length.

For EC3, the low-frequency damage increases from 1.76×10^{-3} (80.5% of total) for 10-minute windows to 2.18×10^{-3} (99.5% of total) for 15-second windows, i.e. a 19% increase in the low-frequency contribution when the window is reduced from 10-minute to 15-second. This shift is a direct consequence of signal segmentation: shorter windows increase the probability that stress excursions are truncated at window boundaries and, as a result, reconstructed through the residual

https://doi.org/10.5194/wes-2026-108
Preprint. Discussion started: 6 July 2026
© Author(s) 2026. CC BY 4.0 License.

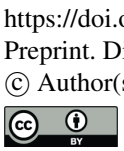

eawe european academy of wind energy
Open Access WIND ENERGY SCIENCE DISCUSSIONS

sequence. With 15-second windows, many stress excursions driven by slowly varying mean loads and operational transitions do not fully close within a single window and are therefore carried into the residual sequence and recovered by residual concatenation. The increase in the low-frequency contribution is thus a redistribution of identified cycles caused by segmentation, rather than a physical increase in low-frequency loading.

For 15-second windows, most fatigue damage is recovered through the residual sequence because short windows reduce the likelihood of stress excursions closing within a single window. Consequently, the suitability of a 15-second window depends on the dominant frequency content of the structural stress response relative to the selected window length, rather than representing a universally optimal choice.

The same trend is observed with the DNV damage model, although the change is larger: for 15-second windows, the low-frequency contribution reaches 97.1% of the total, corresponding to a 27.6% increase relative to 10-minute windows.

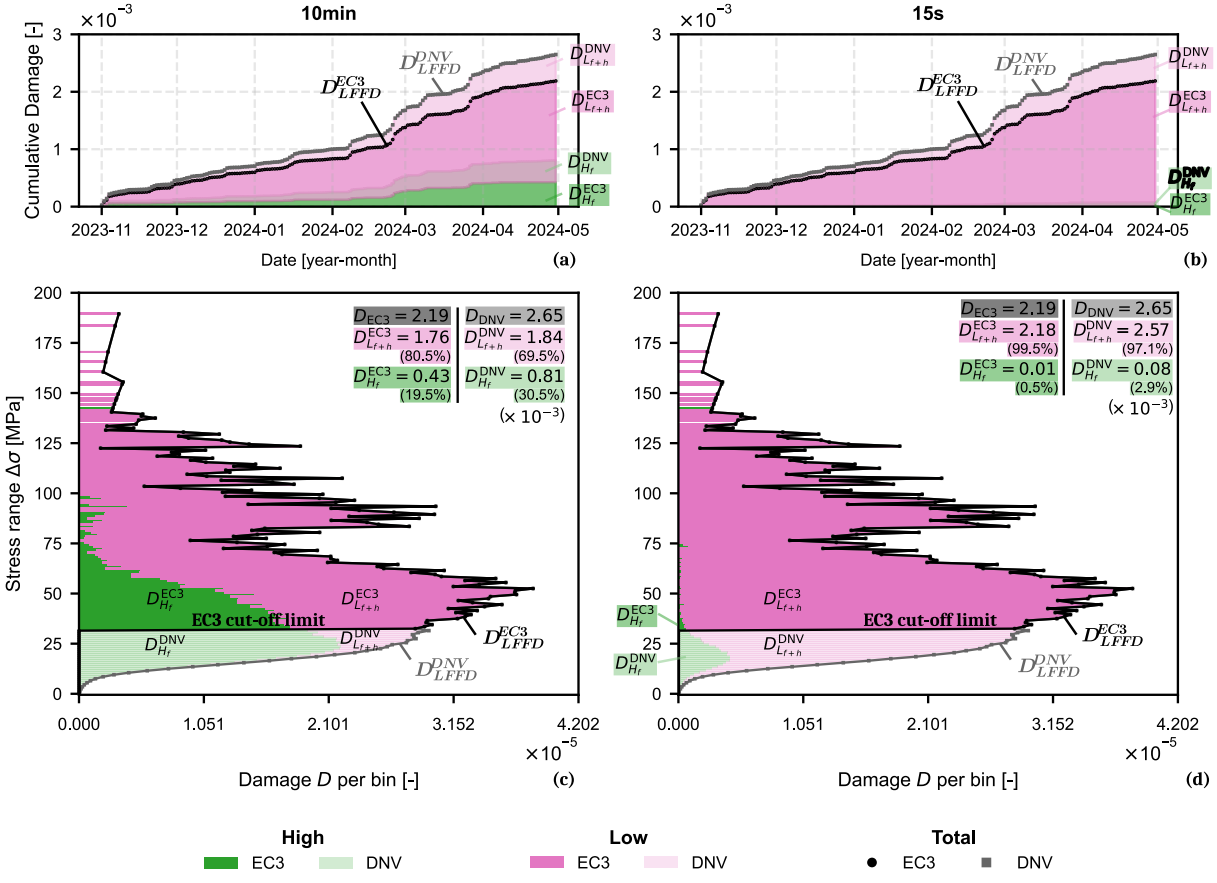

Figure 10. FA-direction fatigue at tower section T1 (six months, 50 Hz). (a–b) Cumulative damage for 10-minute and 15-second windows. (c–d) Final $\Delta\boldsymbol{\sigma} - \boldsymbol{D}$ spectra. Total damage is decomposed into within-window full-cycle damage (green) and residual-based damage (pink). The percentages of damage are computed by Equation (2). Damage is computed using EC3 detail category 80 and DNV welded-steel $\boldsymbol{\sigma} - \boldsymbol{N}$ curves, both employing a bi-linear formulation with slopes $\boldsymbol{m = 3/5}$.

https://doi.org/10.5194/wes-2026-108
Preprint. Discussion started: 6 July 2026
© Author(s) 2026. CC BY 4.0 License.

eawe european academy of wind energy
Open Access WIND ENERGY SCIENCE DISCUSSIONS

4.5 Comparison of Fatigue Monitoring Methods

Having established the influence of window length within a rainflow-equivalent framework, the analysis now turns to reduced-information and window-based methods. Unlike Low-Frequency Fatigue Dynamics (LFFD), these approaches introduce varying degrees of approximation, such that their accuracy reflects both their inherent representation strategy and its interaction with the chosen window length — shorter windows increase reliance on extrema preservation, while longer windows favour within-window cycle closure at the expense of long-period dynamics. Each method is benchmarked against the Low-Frequency Fatigue Dynamics (LFFD) baseline across both window lengths.

To evaluate the combined influence of window length and information reduction on fatigue estimation, four monitoring approaches are compared. These include: (i) the residual-preserving Low-Frequency Fatigue Dynamics (LFFD) methodology, which preserves rainflow equivalence and is adopted as the baseline (Faria et al., 2024; Marsh, 2016; Marsh et al., 2016; Sadeghi et al., 2022, 2023; Shah et al., 2025, 2026); (ii) conventional window based high cycle rainflow counting using fixed window lengths in accordance with IEC practice (IEC 61400-13, 2015); and (iii) two reduced information extrema sequence representations, namely the Start–Peaks–Valleys–End (SPVE) and Maximum–Minimum (Max–Min) methods, which retain only representative stress extrema per window to reduce computational and storage demands (Larsen and Thomsen, 1996; Shah et al., 2025, 2026). These methods span the range from rainflow equivalent fatigue estimation to highly compressed representations, enabling systematic assessment of how window length interacts with different levels of information reduction.

Figure 11 presents cumulative damage and end-of-period $\Delta\sigma - N$ and $\Delta\sigma - D$ spectra for all methods. Differences are most pronounced under 10-minute windowing, where segmentation truncates long-period stress variations and suppresses moderate stress-range content that contributes materially to damage accumulation. The Start–Peaks–Valleys–End (SPVE) sequence reproduces fatigue damage levels very close to the Low-Frequency Fatigue Dynamics (LFFD) baseline for both window lengths, demonstrating that preserving a limited set of representative turning points per window is sufficient to retain most fatigue-relevant information without requiring within-window rainflow counting. In contrast, the Max–Min approach exhibits a strong dependence on window length: under 10-minute windowing, it substantially underestimates fatigue damage due to the loss of moderate-stress-range cycles, whereas for 15-second windows, its agreement with the baseline improves markedly as extrema more accurately represent the underlying turning-point sequence.

https://doi.org/10.5194/wes-2026-108
Preprint. Discussion started: 6 July 2026
© Author(s) 2026. CC BY 4.0 License.

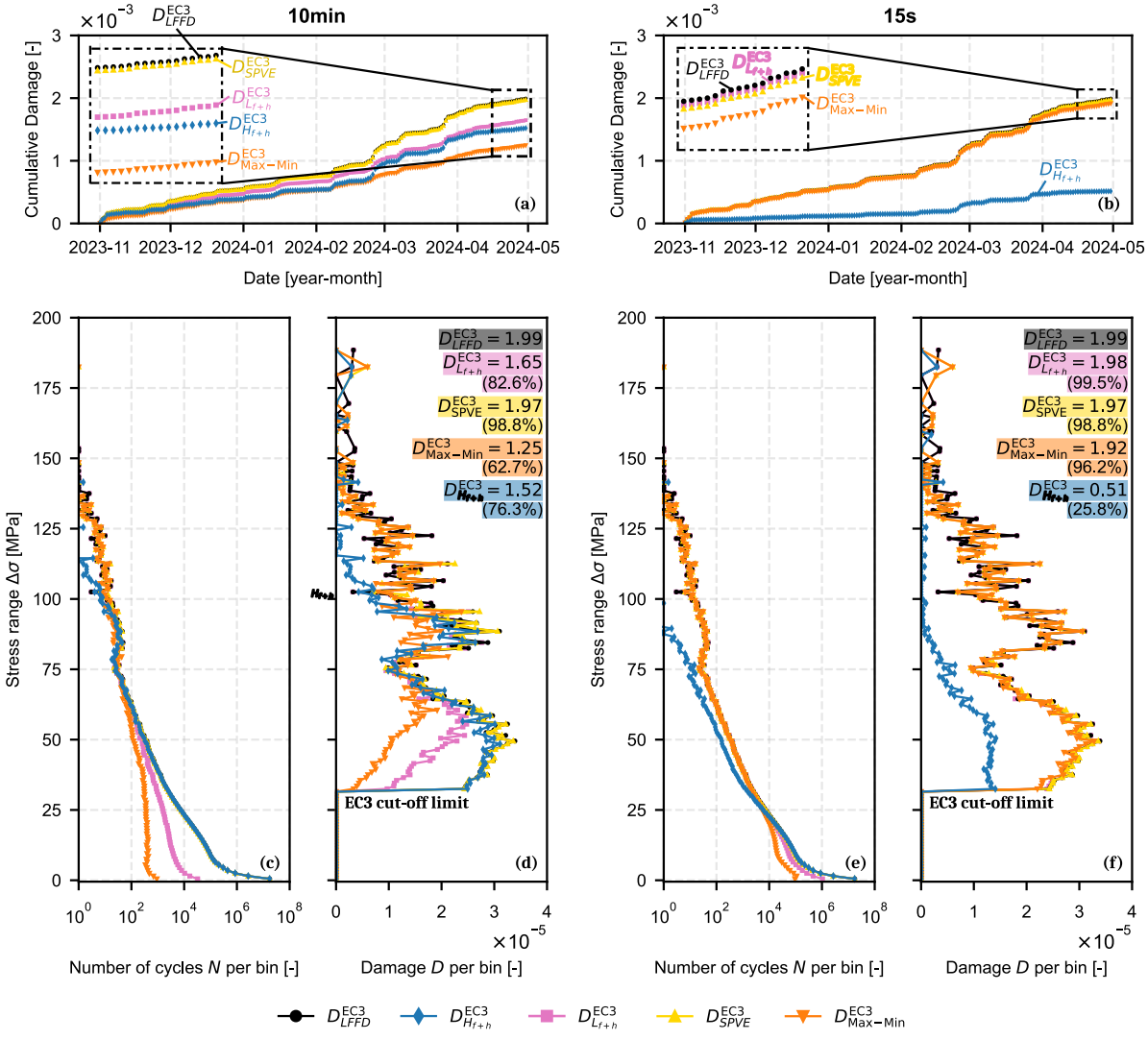

Figure 11. FA-direction fatigue at tower section T1 (six months, 6.25 Hz). (a–b) Cumulative damage for 10-minute and 15-second windows. (c, e) $\Delta\boldsymbol{\sigma} - \boldsymbol{N}$ spectra and (d ,f) $\Delta\boldsymbol{\sigma} - \boldsymbol{D}$ spectra at the end of the six months. Curves compare LFFD total damage (baseline), LFFD low-frequency contribution, Start–Peaks–Valleys–End (SPVE), Max–Min, and conventional window-based high-cycle counting (IEC practice when applied to 10-minute). Percentages indicate total damage relative to the LFFD baseline (Equation (5), EC3). Damage is computed using EC3 detail category 80, employing a bi-linear formulation with slopes $\boldsymbol{m = 3/5}$.

Figure 12 summarises the accuracy of each fatigue monitoring methodology using the damage ratio defined in Equation (5) as a function of window length, and Table 2 places these results in the context of representative literature findings for different fatigue exponents and turbine components. Figure 12a–b compares the performance of the evaluated methods under 10-minute and 15-second windows. High-fidelity fatigue assessment can be achieved using highly compressed stress representations, particularly when short window lengths are adopted. For 15-second windows, both residual-preserving and extrema-based approaches achieve damage ratios close to unity, whereas larger deviations are observed under conventional 10-minute windows due to truncation of long-period stress variations.

https://doi.org/10.5194/wes-2026-108
Preprint. Discussion started: 6 July 2026
© Author(s) 2026. CC BY 4.0 License.

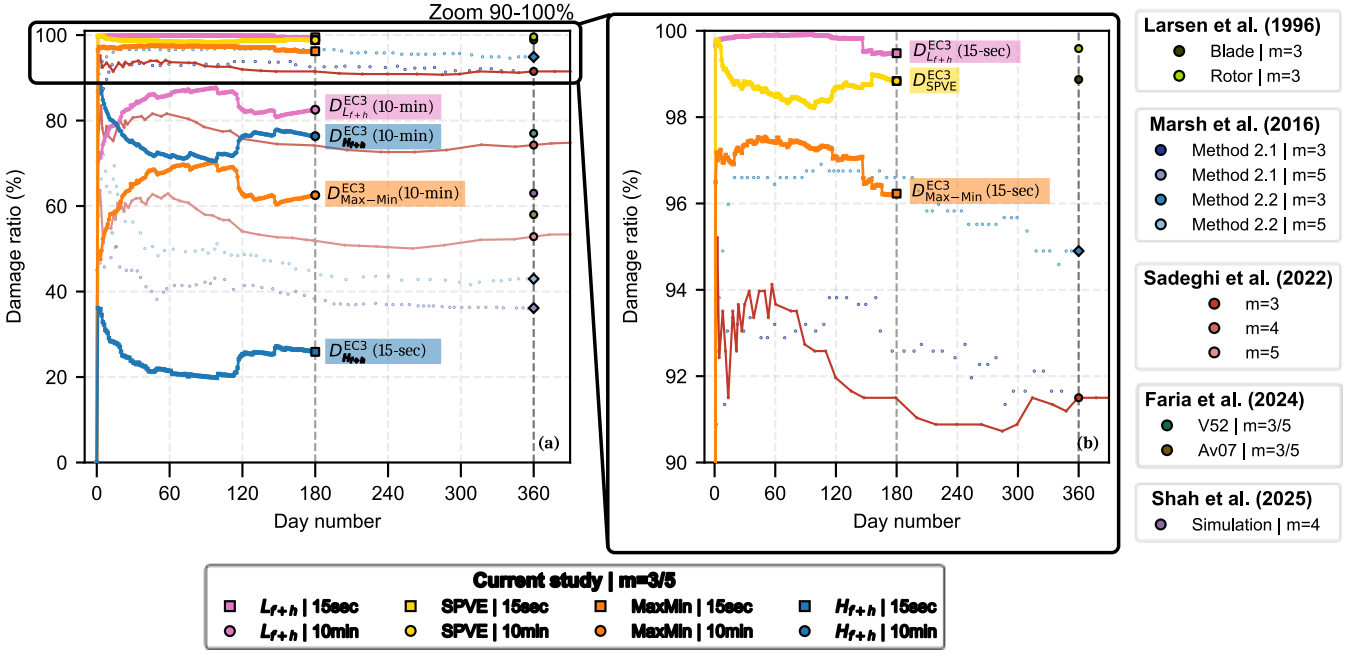

Figure 12. Fatigue damage accuracy as a function of window length, expressed through the damage ratio defined in Equation (5). Values close to 100% indicate agreement with the baseline, while deviations quantify under- or over-estimation due to aggregation and information reduction. Panels (a) and (b) show damage ratios obtained in the present study for 10-minute and 15-second windows, respectively, comparing LFFD, Start–Peaks–Valleys–End (SPVE), Max–Min, and conventional window based high cycle counting.

https://doi.org/10.5194/wes-2026-108
Preprint. Discussion started: 6 July 2026
© Author(s) 2026. CC BY 4.0 License.

Table 2. Comparison of fatigue damage ratios (%) reported in the literature and obtained in the present study for different damage estimation methods, window lengths, and fatigue slopes ($\boldsymbol{m}$) (Faria et al., 2024; Larsen and Thomsen, 1996; Marsh, 2016; Marsh et al., 2016; Sadeghi et al., 2022; Shah et al., 2025). For the current study, values represent the ratio of estimated damage to the continuous rainflow counting baseline defined in Equation (5). For literature studies, values represent the ratio of damage estimated without low-frequency fatigue cycle recovery to the damage estimated with full residual concatenation. Results cover a range of turbine components, modelling approaches, and damage accumulation strategies, providing a benchmark for evaluating the performance of the proposed methods.

Method	Study	Window Length*/Slope of the damage curve m**				
		15-second	10-minute			
		$m = 3/5$	$m = 3$	$m = 3/5$	$m = 4$	$m = 5$
Window-based High-cycle Counting	Sadeghi et al. (2022)	-	91.5	-	74.3	52.8
	Faria et al. (2024) – Av07	-	-	58.0	-	-
	Faria et al. (2024) – V52	-	-	77.0	-	-
	Shah et al. (2025)	-	-	-	63.0	-
	Current study	25.8	-	76.3	-	-
Residual recover	Marsh et al. (2016) - Method 2.1	-	92.0	-	-	37.0
	Marsh et al. (2016) - Method 2.2	-	95.0	-	-	43.0
Residuals Sequence (LFFD Low)	Current study	99.5	-	82.6	-	-
Start–Peaks–Valleys–End (SPVE)	Current study	98.8	-	98.8	-	-
Maximum-Minimum (Max-Min)	Larsen et al. (1996)*** - Blade	-	98.9	-	-	-
	Larsen et al. (1996)*** - Rotor	-	99.6	-	-	-
	Current study	96.2	-	62.7	-	-

*All literature values correspond to 10-minute window lengths unless otherwise indicated.
**The $m = 3/5$ column refers to a bi-linear $\sigma - N$ curve formulation with slopes $m = 3$ and $m = 5$, as used in Eurocode 3 and DNV standards. Single-slope results from the literature ($m = 3$, $m = 4$, $m = 5$) are reported in the respective columns.
***Larsen et al. (1996) values represent the high-frequency damage contribution prior to inclusion of the low-frequency component, applied to blade flapwise and rotor tilt moments using a Max–Min approximation.

Practical deployment at wind-farm scale is constrained not only by estimation accuracy, but also by data-handling and computational requirements. To assess these aspects, each methodology was evaluated using only the data strictly required for its implementation. Retaining only the concatenated residual sequence within the Low-Frequency Fatigue Dynamics (LFFD) framework requires approximately 7% of the raw data volume, while the Maximum-Minimum (Max-Min) representation reduces this further to about 2%, and Start–Peaks–Valleys–End (SPVE) retains roughly 50%. Extrema-based representations further reduce computational complexity by requiring only a single rainflow counting operation on the concatenated reduced sequence, rather than repeated cycle counting at every window. For 15-second windows, Start–Peaks–Valleys–End (SPVE) achieves approximately 99% damage accuracy with around 50% data reduction, while Maximum–Minimum (Max–Min) reaches roughly 96% accuracy while retaining only about 2% of the original data.

The evaluated methodologies are summarised in Table 3 according to required data resolution, damage accuracy, computational effort, and storage requirements. Taken together, these results demonstrate that accurate fatigue estimation can be achieved using highly reduced stress representations when short, SCADA-aligned windows are adopted. Residual-preserving and extrema-based approaches retain the fatigue-relevant information required for rainflow-equivalent damage estimation, while substantially reducing data volume and computational complexity, enabling practical

https://doi.org/10.5194/wes-2026-108
Preprint. Discussion started: 6 July 2026
© Author(s) 2026. CC BY 4.0 License.

implementation of fatigue monitoring at sub-minute resolution using operational SCADA and strain measurements, without requiring continuous high-frequency data storage or processing.

Table 3. Overview of the fatigue assessment methods evaluated in this study, summarising data resolution requirements, computational effort, storage needs, and the comparative characteristics of each method. Computational effort refers to the need to perform rainflow cycle counting repeatedly at the window level versus a single rainflow operation applied to a concatenated reduced information stress sequence.

Method	Required Data Resolution	Damage accuracy	Data storage	Rainflow Count Operations	Computational effort
Window-based High-cycle Counting	10-minute	76.3%	26,209 histograms	Per window	High
Low-Frequency Fatigue Dynamics (LFFD)	10-minute	100%	~7% (residuals sequence) + 26,209 histograms (high)	Per window	High
Residuals Sequence (LFFD Low)	15-second	99.5%	~7% (residuals sequence) + 1 histogram	Per window	High
Start–Peaks–Valleys–End (SPVE)	10-minute/ 15-second	98.8%	~47% (sequence) + 1 histogram	Single	Low
Maximum-Minimum (Max-Min)	15-second	96.2%	~2% (sequence) + 1 histogram	Single	Low

5 Conclusions

This study assessed fatigue-monitoring methodologies suitable for real-time, fleet-scale deployment on wind turbines, using six months of high-frequency tower-strain measurements from an onshore turbine. Rainflow Cycle Counting (RFC) was used as the baseline, against which window-based approaches, the Low-Frequency Fatigue Dynamics (LFFD) method, and two reduced-information extrema-sequence representations, Start–Peaks–Valleys–End (SPVE) and Maximum–Minimum (Max–Min), were benchmarked across multiple sampling rates, window lengths, and two fatigue-curve standards (Eurocode 3 and DNV).

The central question addressed is whether SCADA-aligned short windows can replace the conventional 10-minute standard while preserving fatigue-damage accuracy and remaining practically deployable at scale. The results show that the answer depends critically on the method used. Conventional 10-minute window-based counting recovered only 76.3% of baseline damage due to cycle truncation at boundaries. Reducing the window length to 15 seconds does not resolve this — shorter windows increasingly truncate the low-frequency cycles that dominate fatigue damage, and the window-based method retains only 25.8% of baseline damage at 15-second segmentation. It is the Low-Frequency Fatigue Dynamics (LFFD) formulation that removes this window-length dependence entirely: by explicitly reconstructing inter-window cycles through residual concatenation, it recovers 99.5% of baseline damage regardless of segmentation length. A direct consequence of 15-

https://doi.org/10.5194/wes-2026-108
Preprint. Discussion started: 6 July 2026
© Author(s) 2026. CC BY 4.0 License.

second segmentation is that nearly all fatigue-relevant information migrates to the inter-window residuals, with the low-frequency component accounting for 99.5% of total damage — a redistribution driven by segmentation, not by a physical increase in low-frequency loading.

Among reduced-information methods, Start–Peaks–Valleys–End (SPVE) reproduces 98.8% of baseline damage across both window lengths while reducing stored data by approximately 50% and requires only a single rainflow counting operation, making it well-suited for fleet-level fatigue monitoring. Maximum–Minimum (Max–Min) method achieves 96.2% accuracy at 15-second windows while retaining only ~2% of the raw data, the highest compression among all methods evaluated; however, its accuracy degrades substantially under 10-minute windowing (62.7%), where moderate stress-range cycles are lost. The choice between these two methods, therefore, depends on the deployment context: the Start–Peaks–Valleys–End (SPVE) method is preferable when accuracy is the priority, while the Maximum–Minimum (Max–Min) method is better suited to highly resource-constrained architectures where extreme data compression is required.

Regarding fatigue-curve selection, EC3 estimates 17–66% less accumulated damage than DNV, depending on the tower section, and is identified as the more appropriate standard for the welded tubular steel details of onshore towers. Downsampling from 50 Hz to 12.5–25 Hz introduces negligible deviation; 6.25 Hz offered a practical compromise for scalable architectures with bounded underestimation of up to ~9%.

The original contributions of this work are threefold. First, it provides a systematic comparison of window-based, residual-preserving, and extrema-sequence fatigue-monitoring methods under SCADA-aligned short windows, using real strain data. Second, it demonstrates quantitatively that 15-second SCADA-aligned segmentation, combined with either residual-preserving processing or extrema sequences, enables accurate and data-efficient fatigue monitoring without continuous high-frequency data storage. Third, it establishes that the inter-window residual sequence alone, at only ~7% of the raw data volume, is sufficient to reconstruct reference-equivalent fatigue damage, offering a practical pathway for long-term fleet-scale monitoring.

Future work will apply the proposed 15-second SCADA-aligned fatigue estimation framework to long-term operational data and will explore fatigue prediction at the finest achievable granularity by forecasting extrema sequences, particularly Maximum–Minimum (Max–Min) representations at 15-second resolution. This approach aims to enable predictive fatigue monitoring without requiring continuous high-frequency strain measurements, supporting proactive lifetime management at wind-farm scale.

List of Abbreviations

EC3	Eurocode 3 design standard for steel structures
DNV	DNVGL-RP-C203 recommended practice for fatigue design of offshore and onshore steel structures
FA	Fore–Aft direction of the wind turbine tower

https://doi.org/10.5194/wes-2026-108
Preprint. Discussion started: 6 July 2026
© Author(s) 2026. CC BY 4.0 License.

HF	High-frequency fatigue contribution (cycles closing within a window)
LFFD	Low-Frequency Fatigue Dynamics methodology
LF	Low-frequency fatigue contribution (cycles spanning multiple windows and reconstructed via residuals)
Max-Min	Maximum–Minimum extrema sequence representation
RFC	Rainflow Cycle Counting
SCADA	Supervisory Control and Data Acquisition
SHM	Structural Health Monitoring
SPVE	Start–Peaks–Valleys–End extrema sequence representation
SS	Side-to-Side direction of the wind turbine tower

Data availability

The strain and SCADA measurements used in this study are proprietary data collected under a confidentiality agreement with the industrial partner and cannot be shared publicly.

Author contributions

Conceptualisation, C.O., A.B., J.P.S., and E.C.; methodology, C.O., A.B.; software, C.O.; validation, A.B., J.P.S., and E.C.; formal analysis, C.O., A.B.; investigation, C.O.; resources, A.B.; data curation, C.O.; writing – original draft preparation, C.O., A.B.; writing – review and editing, C.O., A.B., J.P.S., E.C., and M.X.; visualisation, C.O.; supervision, J.P.S., E.C., and M.X.; project administration, A.B. and J.P.S.; funding acquisition, J.P.S.

Competing interests

The authors declare that none of the authors has any conflict of interest.

Acknowledgements

The work is a collaborative research effort between the Faculty of Engineering, University of Porto, Nadara and the National Laboratory for Civil Engineering (LNEC).

https://doi.org/10.5194/wes-2026-108
Preprint. Discussion started: 6 July 2026
© Author(s) 2026. CC BY 4.0 License.

Financial support

This work is funded by the PhD Grant ref. 2021.06078.BD. It is also part of the ongoing research project: "M4WIND – Monitoring, Modelling and Machine learning for Managing the operating life of WIND farms", ref. 2022.08120.PTDC, and Base Funding - UIDB/04708/2020, with DOI 10.54499/UIDB/04708/2020, of CONSTRUCT - Instituto de I&D em Estruturas e Construções, both funded by national funds through FCT/MCTES (PIDDAC).

References

Amzallag, C., Gerey, J. P., Robert, J. L., and Bahuaud, J.: Standardization of the rainflow counting method for fatigue analysis, Int. J. Fatigue, 16, 287–293, https://doi.org/10.1016/0142-1123(94)90343-3, 1994.

Faria, B. R., Sadeghi, N., Dimitrov, N., Kolios, A., and Abrahamsen, A. B.: Inclusion of low-frequency cycles on tower fatigue lifetime assessment through relevant environmental and operational conditions, in: Journal of Physics: Conference Series, https://doi.org/10.1088/1742-6596/2767/4/042021, 2024.

HBM: Strain Gauges 1-LY11-10/350, 2022.

IEC 61400-12-1: Wind turbines-Part 12-1: Power performance measurements of electricity producing wind turbines, IEC 61400-12-1, 2005.

IEC 61400-13: Wind turbines - Part 13: Measurement of mechanical loads., 1.0., International Electrotechnical Commission, 219 pp., 2015.

Kauzlarich, J. J.: The Palmgren-Miner rule derived, in: Tribology Series, vol. 14, Elsevier, 175–179, 1989.

Larsen, G. C. and Thomsen, K.: Low cycle fatigue loads, Risø-R-913(EN), Roskilde, Denmark, 1996.

Marsh, G.: Fatigue Load Monitoring of Offshore Wind Turbine Support Structures, 2016.

Marsh, G., Wignall, C., Thies, P. R., Barltrop, N., Incecik, A., Venugopal, V., and Johanning, L.: Review and application of Rainflow residue processing techniques for accurate fatigue damage estimation, Int. J. Fatigue, 82, 757–765, https://doi.org/10.1016/j.ijfatigue.2015.10.007, 2016.

Matsuishi, M. and Endo, T.: Fatigue of metals subjected to varying stress, Japan society of mechanical engineers, 68, 37–40, 1968.

McInnes, C. H. and Meehan, P. A.: Equivalence of four-point and three-point rainflow cycle counting algorithms, Int. J. Fatigue, 30, 547–559, https://doi.org/10.1016/j.ijfatigue.2007.03.006, 2008.

Miner, M. A.: Cumulative Damage in Fatigue, J. Appl. Mech., 12, A159–A164, https://doi.org/10.1115/1.4009458, 1945.

Oliveira, C., Biscaya, A., Santos, J., Caetano, E., and Xu, M.: Low-frequency fatigue dynamics estimation of a wind turbine tower: a comparison using 10-minute and high-frequency data, J. Phys. Conf. Ser., 3224, 072018, https://doi.org/10.1088/1742-6596/3224/7/072018, 2026.

Pacheco, J., Pimenta, F., Pereira, S., Cunha, Á., and Magalhães, F.: Fatigue Assessment of Wind Turbine Towers: Review of Processing Strategies with Illustrative Case Study, https://doi.org/10.3390/en15134782, 2022.

https://doi.org/10.5194/wes-2026-108
Preprint. Discussion started: 6 July 2026
© Author(s) 2026. CC BY 4.0 License.

Pacheco, J. M. S.: Development of New Methodologies for Structural Monitoring of Wind Farms, Faculdade de Engenharia da Universidade do Porto, Porto, Portugal, 2022.

Sadeghi, N., Robbelein, K., D'Antuono, P., Noppe, N., Weijtjens, W., and Devriendt, C.: Fatigue damage calculation of offshore wind turbines' long-term data considering the low-frequency fatigue dynamics, in: Journal of Physics: Conference Series, https://doi.org/10.1088/1742-6596/2265/3/032063, 2022.

Sadeghi, N., D'Antuono, P., Noppe, N., Robbelein, K., Weijtjens, W., and Devriendt, C.: Quantifying the effect of low-frequency fatigue dynamics on offshore wind turbine foundations: a comparative study, Wind Energy Science, 8, 1839–1852, https://doi.org/10.5194/wes-8-1839-2023, 2023.

Shah, A. H., Vad, A., Guilloré, A., and Bottasso, C. L.: Towards a load surrogate model for low-frequency fatigue cycles in wind turbines, in: Wind Energy Science Conference, https://doi.org/10.1088/1742-6596/2767/3/032019, 2025.

Shah, A. H., Vad, A., Guilloré, A., and Bottasso, C. L.: Towards a load surrogate model for low-frequency fatigue cycles in wind turbines, J. Phys. Conf. Ser., 3224, 062064, https://doi.org/10.1088/1742-6596/3224/6/062064, 2026.